Received: 1 August 2024 | Revised: 6 September 2024 | Accepted: 9 September 2024

DOI: 10.1002/ardp.202400618

ARCH PHARM DPhG
Archiv der Pharmazie

FULL PAPER

Evaluation of the effect of carvedilol orodispersible tablets on ischemia–reperfusion injury and flap viability in rats: An in vivo study

Serkan Tokgonul[1] | Emine Dilek Ozyilmaz[2] | Tansel Comoglu[3] | Manolya Müjgan Gürbüz[4,5] | Burcu Doğan Topal[6] | Fatma Emel Kocak[7] | Hülda Rıfat Ozakpinar[1]

[1]Plastic Surgery Clinic, Etlik City Hospital, Ankara, Turkey

[2]Faculty of Pharmacy, Department of Pharmaceutical Technology, Eastern Mediterranean University, Famagusta, North Cyprus, Turkey

[3]Department of Pharmaceutical Technology, Faculty of Pharmacy, Ankara University, Ankara, Turkey

[4]Institute of Health Sciences, Ankara University, Ankara, Turkey

[5]Department of Analytical Chemistry, Faculty of Pharmacy, Medipol University, Ankara, Turkey

[6]Department of Analytical Chemistry, Faculty of Pharmacy, Ankara University, Ankara, Turkey

[7]Department of Medical Biochemistry, Faculty of Medicine, Kütahya Health Sciences University, Kutahya, Turkey

Correspondence
Tansel Comoglu, Department of Pharmaceutical Technology, Faculty of Pharmacy, Ankara University, Ankara, Turkey.
Email: comoglu@pharmacy.ankara.edu.tr

Funding information
None

Abstract

Flap surgery is an integral part of plastic surgery, and ischemia–reperfusion (I/R) injury significantly affects the viability of the flap. Carvedilol (CRV), a nonselective beta-blocker with alpha-1 blocking and antioxidant properties, and known for its potential in reducing I/R damage, was chosen as the active substance for our study. The aim of this study was to investigate the vasodilator and antioxidant effects of CRV on rat inferior epigastric artery skin flap using orally disintegrating tablets (ODTs). The optimized ODT formulation was subjected to in vivo experiments using Sprague–Dawley female rats (n = 24) divided into three groups: Group I (control, I/R), Group II (treatment, I/R + CRV), and Group III (treatment, I/R), I/R + CRV ODT). Reperfusion was then observed following the release of the microclamp from the pedicle, and the flap was then re-adapted to its original position. Control rats were given oral isotonic solution via gavage and were subjected to 8 h of ischemia and 12 h of reperfusion. Group II was given 2 mg/kg CRV oral tablets for 7 days before and after surgery. Group III was given 2 mg/kg/day CRV ODT for the same period. Biopsies were taken from the flap and histopathological and biochemical analyses including superoxide dismutase, glutathionenitric oxide, malondialdehyde, para-oxonase 1, total oxidant, and total antioxidant capacities were performed. This study demonstrates that CRV ODTs significantly increased flap viability by approximately 25% compared to the control group, highlighting their promising therapeutic potential.

KEYWORDS
carvedilol, flap viability, ischemia–reperfusion injury, orodispersible tablets

Serkan Tokgonul and Emine Dilek Özyılmaz have equal shares in this study.

1 | INTRODUCTION

Flap surgery, an essential part of plastic surgery, involves transferring tissue from one area of the body to another, playing a critical role in reconstructive procedures. However, the success of flap surgeries is closely linked to the challenges posed by ischemia–reperfusion (I/R) injury, where blood flow is temporarily interrupted and then restored, affecting the viability of the transferred tissue.[1]

Carvedilol (CRV) is a pharmaceutical agent with diverse effects, attracting significant interest due to its dual action as a nonselective beta-blocker and an alpha-1 blocker, alongside its intrinsic antioxidant properties. This unique pharmacological profile transcends its conventional role in cardiovascular conditions, suggesting a promising role in mitigating the detrimental effects of I/R injury in flap surgery. CRV's effectiveness as a nonselective beta-blocker stems from its ability to bind to both beta-1 and beta-2 adrenergic receptors, thereby inhibiting the stimulating effects of catecholamines. This action reduces heart rate and contractility, lowering blood pressure and workload, particularly beneficial in managing conditions like hypertension and heart failure.[2,3] Furthermore, CRV's alpha-1 blocking activity promotes vasodilation by inhibiting the α1-adrenergic receptors in vascular smooth muscle cells. This leads to increased blood flow, which is crucial for tissue perfusion and oxygen delivery, particularly vital in the context of flap surgery where tissue viability is paramount.[4]

Adding to its repertoire, CRV possesses intrinsic antioxidant properties. This attribute stems from its ability to scavenge free radicals and reactive oxygen species (ROS) generated during I/R injury. ROS contribute to cellular damage, tissue necrosis, and impaired flap survival. By neutralizing these harmful molecules, CRV offers additional protection against I/R-induced tissue injury. Several studies have investigated the effectiveness of CRV in mitigating I/R injury and improving flap survival in diverse animal models.[5]

Given its dual action, we hypothesize that CRV, particularly in an ODT formulation, will enhance flap viability by reducing oxidative stress and improving blood flow during I/R injury.

A study published in the *Journal of Plastic, Reconstructive & Aesthetic Surgery* (2017) demonstrated that CRV administration significantly improved flap survival in a rat model of I/R injury. The treated group showed increased blood flow, reduced tissue necrosis, and better histological outcomes compared to the control group.[6]

Another study published in *Microsurgery* (2014) investigated the effects of CRV in a microsurgical model of I/R injury. The results showed that CRV treatment significantly reduced muscle fiber degeneration and necrosis, preserving tissue integrity and enhancing muscle function.[7]

A study investigated the antioxidant effects of CRV in a rabbit model of I/R injury. The study demonstrated that CRV significantly reduced ROS levels and lipid peroxidation in the flap tissue, suggesting its potential to mitigate oxidative damage and improve flap survival.[8]

These studies, along with others, provide promising evidence for the potential of CRV as a therapeutic agent in mitigating I/R injury and improving flap survival in surgery. Further research, particularly clinical trials, is warranted to confirm these findings and establish CRV's definitive role in improving surgical outcomes.

The focus of this study is to delve into the vasodilatory and antioxidant facets of CRV within the context of rat inferior epigastric artery skin flaps. To enhance its pharmacological profile and facilitate administration, CRV was formulated into orodispersible tablets (ODTs). ODTs, designed to disintegrate rapidly upon contact with saliva, offer a convenient and patient-friendly means of drug delivery.

The formulation of CRV into ODTs offers several key advantages over traditional tablets, including improved bioavailability, faster disintegration, and enhanced patient compliance, especially in situations where rapid drug delivery is required. ODTs mitigate the challenges some patients face with swallowing traditional tablets, especially when rapid drug delivery is needed. This characteristic is especially advantageous in clinical settings requiring immediate action, such as in emergency situations or for patients with compromised swallowing abilities. Additionally, ODTs offer improved bioavailability by enhancing the dissolution rate of CRV, promoting quicker absorption and onset of therapeutic action. The patient-friendly nature of ODTs aligns with enhanced compliance, as they provide a palatable and easily ingestible alternative to conventional tablets, particularly for individuals with preferences or restrictions related to tablet swallowing.[9–11] These attributes collectively underscore the significance of ODTs in optimizing the pharmacological profile of CRV for improved patient outcomes in the specific context of rat inferior epigastric artery skin flaps and I/R injury.

Flap surgery, an integral component of plastic surgery, stands as a linchpin in reconstructive procedures, yet its success is often marred by the challenges posed by I/R injury. Despite these challenges, there is limited research on the efficacy of ODT formulations of CRV in mitigating I/R injury, which this study aims to address. This study takes a pioneering stride into the domain of rat inferior epigastric artery skin flaps, seeking a nuanced comprehension of CRV's vasodilatory and antioxidant dynamics when presented in ODT form. The formulation of CRV into ODTs, designed for rapid disintegration upon contact with saliva, represents a strategic departure from conventional tablets, introducing a host of advantages. As we delve into the realm of rat models and the intricate paradigm of inferior epigastric artery skin flaps, the focus extends beyond mere drug delivery to unravel how CRV, in its ODT manifestation, orchestrates the intricate interplay between vasodilation and antioxidant defense mechanisms amid the challenges posed by I/R.[12,13]

The implications of this investigation extend far beyond the confines of the laboratory. The outcomes hold the potential to reshape our understanding of surgical outcomes in flap procedures, introducing a new dimension to the therapeutic landscape of plastic surgery. Beyond its conventional cardiovascular applications, the study foresees CRV carving a niche in plastic surgery, offering novel avenues to optimize outcomes in the delicate balance of tissue transfer and ischemic challenges. This exploration bridges

the realms of pharmacology and surgical practice, paving the way for the expanded application of CRV in plastic surgery scenarios, where its vasodilatory and antioxidant attributes might prove transformative.

2 | RESULTS AND DİSCUSSİON

2.1 | Results of the preparation and ın vitro characterization of ADTs containing CRV-β-CD inclusion complex with Box–Behnken experimental design

2.1.1 | Determination of the calibration equation for CRV using UV spectrophotometric method

The calibration equation obtained with the absorbance values measured by UV spectrophotometer of seven different concentrations of CRV solutions prepared as previously described is shown in Figure 1. The optimum parameters of the method are shown in Table 1.

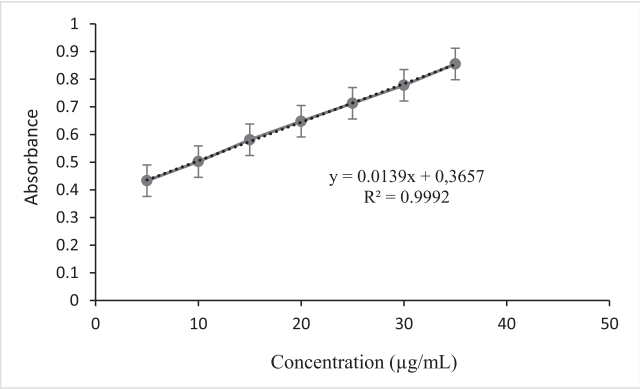

FIGURE 1 Calibration curve of CRV obtained by UV spectrophotometric method. CRV, carvedilol.

TABLE 1 The optimum parameters of the spectrophotometric method.

Parameters	Data
λ_{max}	240 nm
Limit	5–35 µg/mL
Regression equation	$y = 0.0139x + 0.3657$
Correlation coefficient	0.9992
Slope	0.0139
Intercept	0.3657
LOD	0.947 µg/mL
LOQ	1.19 µg/mL

Abbreviations: LOD, limit of detection; LOQ, limit of quantification.

2.1.2 | Preparation and characterization studies of CRV-β-CD inclusion complexes

The solubility of the inclusion complexes prepared by the kneading method was determined by Fourier-transform infrared (FTIR) analyses. Figure 2 shows the FTIR spectra of the inclusion complexes, and Figure 3 and Table 2 show their solubility in aqueous media.

2.1.3 | Preparation and optimization of CRV-β-CD ODT formulations according to Box–Behnken experimental design

After it was determined that the complex that increased the solubility of CRV in the free state the most was 1:3 CRV-β-CD complex, ODTs were prepared using inclusion complexes prepared in this molar ratio and hardness, disintegration time, and friability values were determined. The percentages of mannitol, Parteck ODT®, and magnesium stearate used in the preparation of ODT were determined as independent variables, and hardness, disintegration time, and friability values were determined as dependent variables. The variation of dependent variables versus independent variables is shown in Table 3.

In the prepared ODT formulations, the percentage of mannitol, superdisintegrant (Parteck ODT®), and lubricant (magnesium stearate) were selected as independent variables, while the disintegration time, friability, and hardness values of ODTs were selected as dependent variables. Box–Bhenken experimental design was used to examine the effect of independent variables on dependent variables. In this way, the effect of the independent variables was determined statistically and the percentage amounts of tablet components required for optimum ODT formulation were determined. Table 4 shows the statistical relationship of disintegration time, Table 5 shows tablet hardness, and Table 6 shows percentage friability with the independent variables.

As a result of the evaluations based on the ANOVA data, the three optimized ODT formulations are shown in Table 7.

2.2 | Analytical method development and validation for CRV analysis from biological material

2.2.1 | The results of analytical method development and validation for CRV

In voltammetric bioanalysis, protein precipitation with methanol is a simpler sample pretreatment method that does not require high volumes of organic solvents, expensive instrumentation, and time-consuming sample preparation protocols compared to chromatographic methods. The effect of pH on the voltammetric peak of CRV was performed on a glassy carbon electrode by adsorptive stripping differential pulse voltammetry (AdSDPV) at constant accumulation potential of 0.0 V and accumulation time of 60 s in sulfuric acid (0.1 and 0.2 M) supporting electrolyte, and phosphate buffers (pH 1.5, 3.0, 6.0, 7.0, and 8.0).

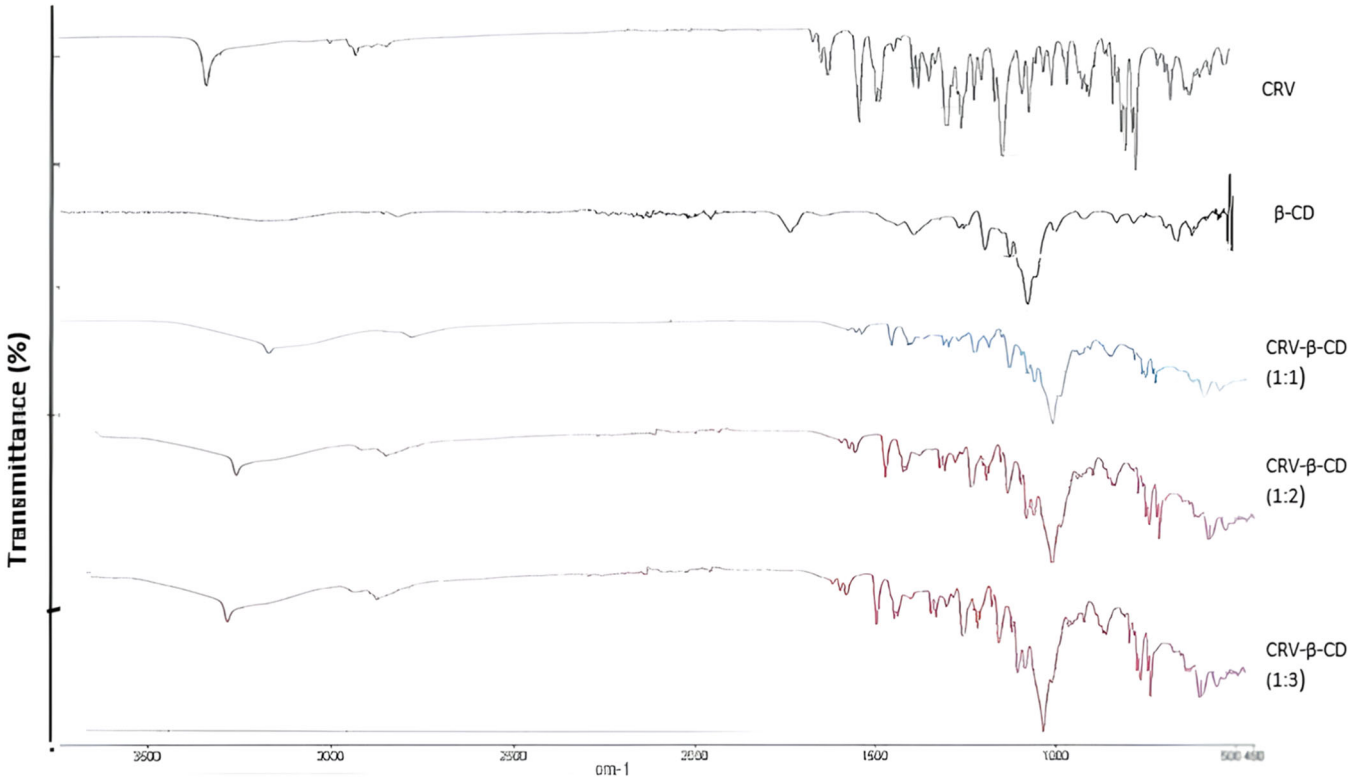

FIGURE 2 FTIR spectra of CRV, β-CD, and inclusion complexes prepared in three different molar ratios (1:1, 1:2, and 1:3). CRV, carvedilol; FTIR, Fourier-transform infrared.

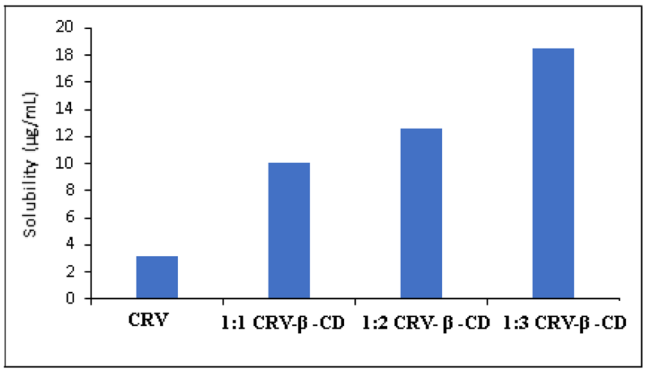

FIGURE 3 Solubility values of CRV and CRV-β-CD complexes. CRV, carvedilol.

TABLE 2 Solubility values obtained from inclusion complexes and rates of increase in solubility.

Sample	C (µg/mL)	Increased solubility (%)
CRV	3.18	-
CRV-β-CD (1:1)	10.02	3.14
CRV-β-CD (1:2)	12.61	3.96
CRV-β-CD (1:3)	18.44	5.79

Abbreviation: CRV, carvedilol.

The maximum peak current value was obtained in phosphate buffer pH 8.02. The peak potential of CRV was shifted to less positive potential with increasing pH indicating the changes in the acid–base protonation functions in drug molecule. The obtained peaks are shown in Figure 4.

The effect of accumulation potential and time on the voltammetric peak current of CRV were evaluated by AdSDPV. When the accumulation time was constant at 60 s, the accumulation potential varied in the range of 0.0–1.0 V. The 0.6 V was chosen because of the higher peak currents. Then the accumulation time was varied in the range of 0–60 min, and 40 min was selected. AdSDPV method was developed and validated for the quantification of CRV in rat serum in phosphate buffer with pH 8.02, based on the optimized conditions. The analytical method validation parameters (limit of detection [LOD], limit of quantification [LOQ], linearity, precision, and accuracy) were calculated according to ICH guidelines (reference ICH Q2). The linearity of calibration curves was observed in the range from 0.17 to 0.34 µg/mL CRV in rat serum (Figure 5). The equation was obtained as ip (µA) = 0.6484 C (mM)–0.0979 (r: 0.9955, n = 5).

LOD and LOQ values were calculated to be 0.037 and 0.112 µg/mL. The intra-day and inter-day variability presented with the %RSD values were found to be 13.14% and 17.59%, respectively. Recovery studies were performed by standard addition method. The recovery values for Group II and Group III rat serum were calculated at 99.83% and 115.63%, respectively. The assay performance data was found as required in the ICH guidelines. The accuracy results showed no significant matrix effects.

TABLE 3 Effect of independent variables on dependent variables.

Run	Factor 1 A: Mannitol (%)	Factor 2 B: Parteck ODT® (%)	Factor 3 C: Magnesium stearate (%)	Response 1 Disintegration time (s)	Response 2 Hardness (N)	Response 3 Friability (%)
1	30	15	1.5	12	35	0.1
2	25	5	1	31	28	0.5
3	30	5	1.5	28	27	0.7
4	25	10	1.5	24	32	0.6
5	35	10	1.5	23	30	0.7
6	30	10	1	20	31	0.9
7	35	15	1	9	30	0.2
8	35	5	1	33	24	0.7
9	30	5	0.5	35	25	0.6
10	25	10	0.5	24	27	0.9
11	35	10	0.5	26	28	0.8
12	30	10	1	25	30	0.8
13	25	15	1	10	35	0.1
14	30	15	0.5	11	37	0.3
15	30	10	1	21	32	0.9

TABLE 4 Statistical relationship of the disintegration time of ODTs with independent variables.

Model	913.75	3	304.58	50.78	<0.0001	Significant
A-Mannitol	0.5000	1	0.5000	0.0834	0.7782	
B-Parteck ODT®	903.13	1	903.13	150.56	<0.0001	
C-Magnesium stearate	10.13	1	10.13	1.69	0.2204	
Residual	65.98	11	6.00			
Lack of Fit	51.98	9	5.78	0.8251	0.6581	Not significant
Pure error	14.00	2	7.00			
Cor total	979.73	14				

Abbreviation: ODT, orodispersible tablet.

TABLE 5 Statistical relationship of ODT hardness with independent variables.

Model	203.75	3	67.92	17.30	0.0002	Significant
A-Mannitol	1.13	1	1.13	0.2866	0.6031	
B-Parteck ODT®	12.50	1	12.50	3.18	0.1019	
C-Magnesium stearate	190.13	1	190.13	48.43	<0.0001	
Residual	43.18	11	3.93			
Lack of fit	41.18	9	4.58	4.58	0.1922	Not significant
Pure error	2.00	2	1.0000			
Cor total	246.93	14				

Abbreviation: ODT, orodispersible tablet.

TABLE 6 Statistical relationship of ODT percentage friability with independent variables.

Model	1.13	9	0.1258	7.47	0.0197	Significant
A-Mannitol	0.0012	1	0.0012	0.0743	0.7961	
B-Parteck ODT®	0.4513	1	0.4513	26.81	0.0035	
C-Magnesium stearate	0.1800	1	0.1800	10.69	0.0222	
Residual	0.0842	5	0.0168			
Lack of fit	0.0775	3	0.0258	7.75	0.1164	Not significant
Pure error	0.0067	2	0.0033			
Cor total	1.22	14				

Abbreviation: ODT, orodispersible tablet.

TABLE 7 Optimized ODT formulations according to the Box–Bhenken experimental design.

Number	Mannitol (%)	Partect ODT® (%)	Magnesium stearate (%)	Desirability	
1	**25**	**15**	**1.5**	**0.978**	**Selected**
2	25.098	15	1.5	0.978	
3	25.17	15	1.5	0.978	

Abbreviation: ODT, orodispersible tablet.

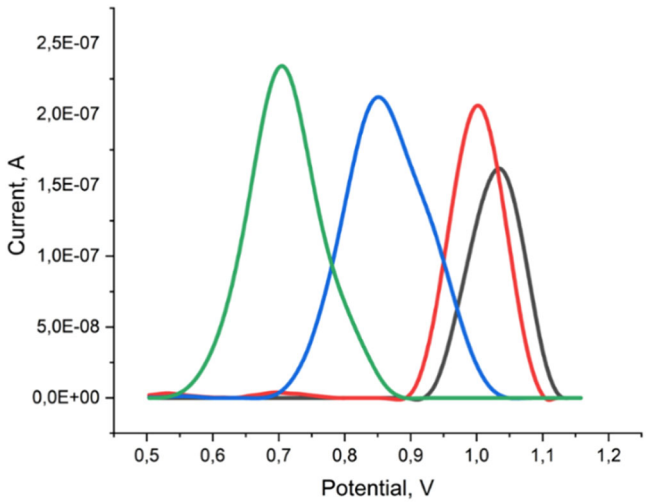

FIGURE 4 The AdSDP voltammograms of CRV on GCE in 0.2 M sulfuric acid supporting electrolyte (black) and phosphate buffer solutions in pH 1.5 (red), pH 6.0 (blue), and pH 8.0 (green). CRV, carvedilol; GCE, glassy carbon electrode.

2.2.2 | CRV analysis from biological material

The validated method was able to quantify CRV in rat serum samples. The serum samples were taken from rats not treated: Group I, treated with CRV: Group II, and treated with CRV-β-CD Inclusion Complexes: Group III. The AdSDP voltammograms of Groups I, II, and III are shown in Figure 6. The peak current of CRV was higher in Group III treated with CRV-β-CD Inclusion Complexes. No voltammetric peak was observed with Group I. It is concluded that the serum concentration level of CRV-β-CD Inclusion formulation was higher than pure CRV formulation.

These voltammetric results were confirmed by statistical analysis based on mean serum concentration with standard deviations for Groups I, II, and III (Figure 7). The values were found to be parametrically distributed. One-way ANOVA test was applied for comparison of mean values (Table 8). Comparison of means between groups was statistically significant ($p < 0.001$). Since the groups were homogeneous, Tukey test was applied. The results of Tukey's test were as follows: there is a statistically significant difference between Groups I and II ($p < 0.001$); there is a significant difference between Groups I and III ($p < 0.001$); there is a significant difference between Groups II and III ($p = 0.042$).

2.3 | In vivo study results

A total of 24 rats were used in the study, and there was no subject loss during the study. No signs of infection were observed in any of the subjects in the postoperative period. There was one flap loss in the control group. Figure 8 shows the images of the rats in which the flaps were placed.

2.3.1 | Biochemical results of tissue and blood samples

Malondialdehyde (MDA) values measured from plasma and tissue samples taken after sacrification are shown in Tables 9 and 10.

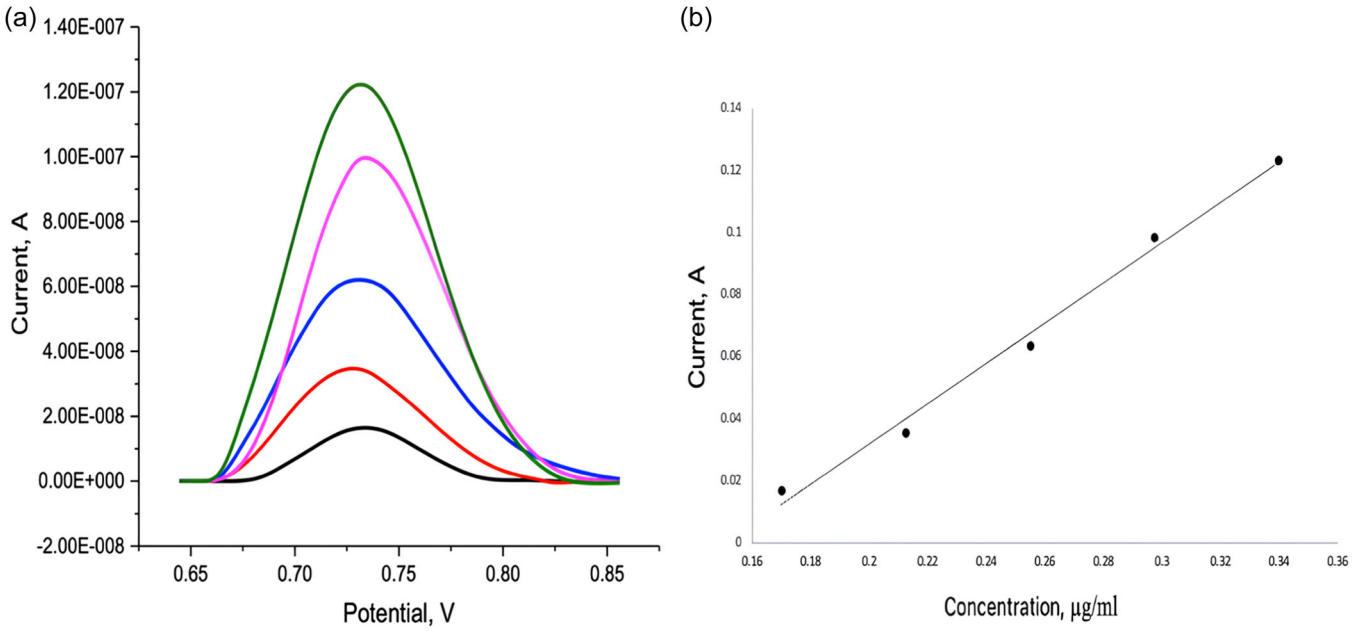

FIGURE 5 AdSDP voltammograms of carvedilol (CRV) concentration levels of 0.17 µg/mL (black), 0.21 µg/mL (red), 0.26 µg/mL (blue), 0.30 µg/mL (pink), and 0.34 µg/mL (green) (a) and calibration graph of CRV concentration levels (b) in rat serum.

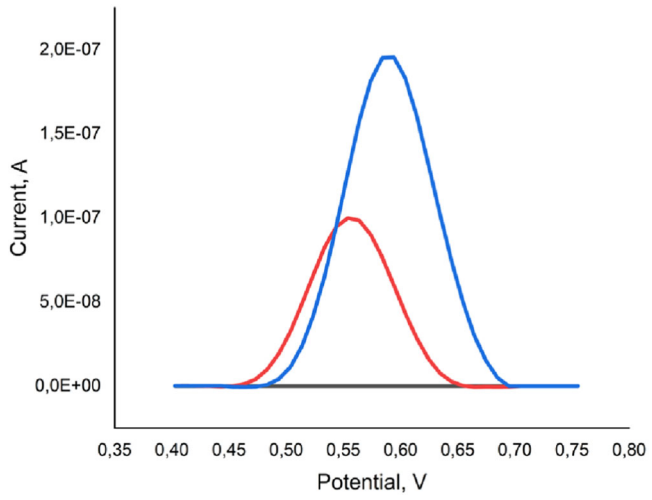

FIGURE 6 AdSDP voltammograms of Group I (black), Group II (red), and Group II (blue) rat serum samples.

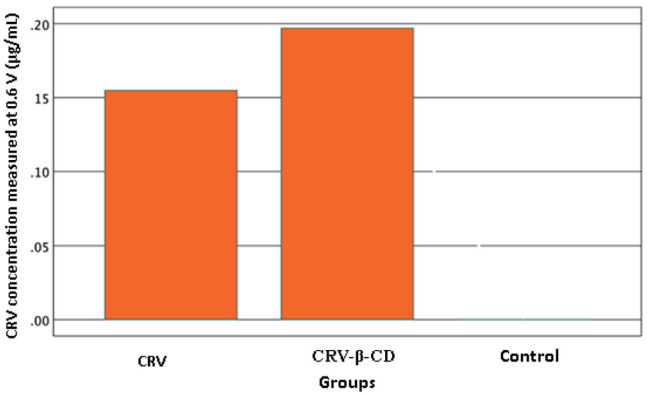

FIGURE 7 The mean serum concentration of CRV after administration of CRV and CRV-β-CD. CRV, carvedilol.

TABLE 8 Results of statistical analysis.

Groups	*N* (number of rat)	Mean serum concentration	Standard deviation	Statistical results
I	7	0	0	$F = 16.203$
II	8	0.1549	0.003	$^{*}p < 0.001$ $^{**}p = 0.042$
III	8	0.1970	0.043	

The means, standard deviations, *p* values, and effect size (η^2) of the MDA data of the groups are shown in Tables 11 and 12.

Nitric oxide (NO) values measured from plasma and tissue samples are shown in Tables 13 and 14. Means, standard deviations, *p* values, and effect size of NO data of the groups are shown in Tables 15 and 16.

As seen in Tables 13–16, nitric oxide levels in Group 3 were significantly higher than in the control group ($p < 0.001$), indicating increased vascular function.

Superoxide dismutase (SOD) values measured from plasma and tissue samples taken after sacrification are shown in Tables 17 and 18.

The means, standard deviations, p values, and effect size of the SOD data of the groups are shown in Tables 19 and 20.

When plasma SOD values of different groups are compared in Table 19, no significant difference ($p = 0.927$) was observed in oxidative stress. However, in Table 20, a significant difference

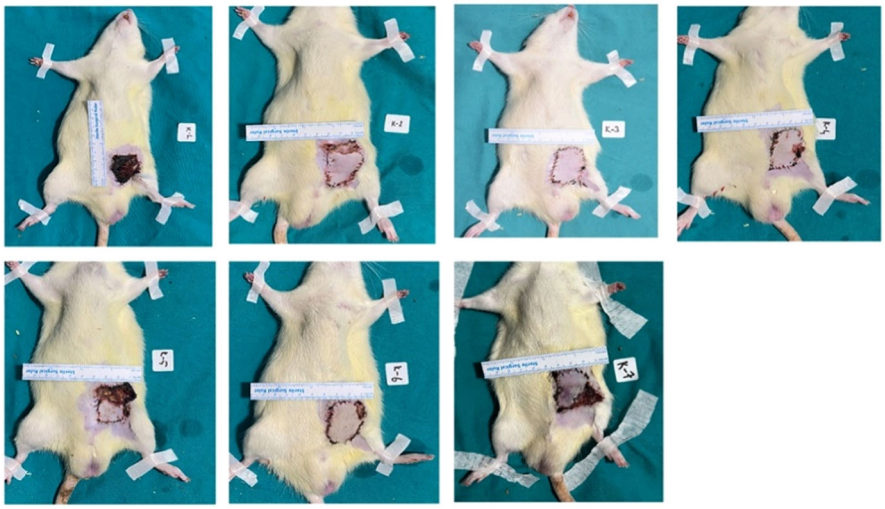

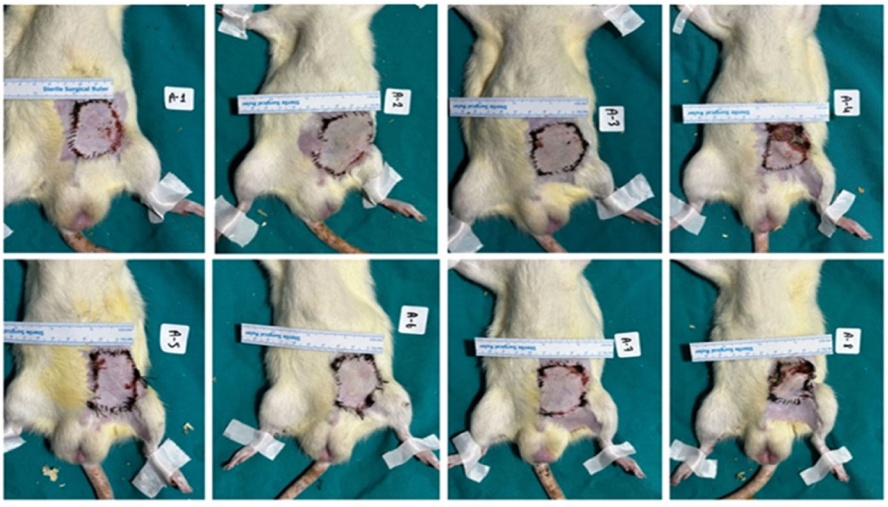

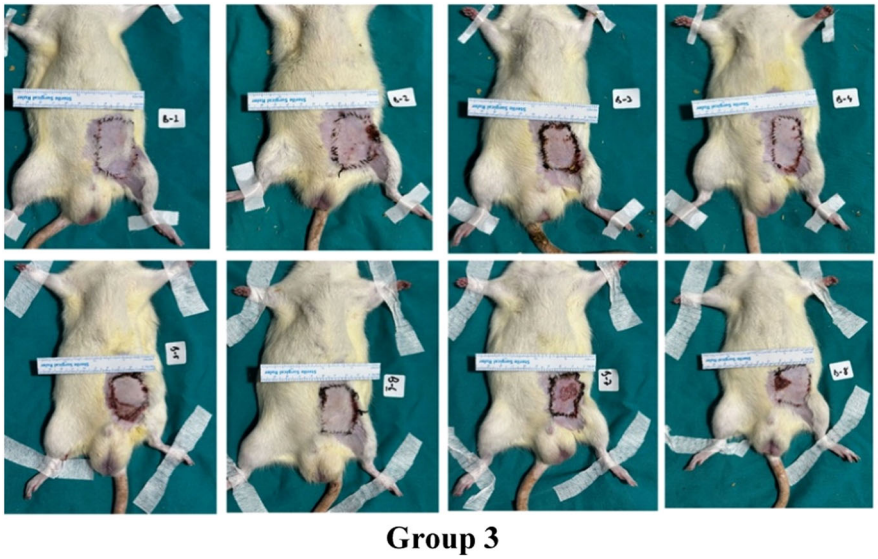

FIGURE 8 Flap implanted rat groups.

TABLE 9 Plasma MDA values.

Plasma MDA	Group 1	Group 2	Group 3
1	25.50	7.37	3.27
2	18.70	3.93	4.88
3	19.55	8.42	3.45
4	9.32	8.10	7.07
5	8.56	7.03	6.05
6	10.16	2.47	6.58
7	9.46	4.63	4.10

Abbreviation: MDA, malondialdehyde.

TABLE 10 Tissue MDA values.

Tissue MDA	Group 1	Group 2	Group 3
1	20.42	19.52	20.80
2	16.60	22.37	35.14
3	26.69	32.17	45.73
4	8.35	13.79	50.66
5	5.47	31.98	13.37
6	30.49	20.33	24.26
7	17.93	14.08	7.51

Abbreviation: MDA, malondialdehyde.

TABLE 11 Comparison of plasma MDA data.

Statistical evaluation of plasma MDA values					
Groups	*N*	Average	Standard deviation	Test statistic	Impact
1	7	14.4571	6.72104	$F = 11.966$	0.545
2	7	5.6075	2.39226	$^{*}p = 0.036$ $^{**}p = 0032$	
3	7	5.3250	1.60927	$^{***}p = 0.990$	

Abbreviation: MDA, malondialdehyde.

TABLE 12 Comparison of tissue MDA data.

Statistical evaluation of tissue MDA values					
Groups	*N*	Average	Standard deviation	Test statistic	Impact
1	7	17.9929	9.03199	$F = 1.143$	0.103
2	7	21.4663	7.17433	$p = 0.339$	
3	7	26.7200	15.59546		

Abbreviation: MDA, malondialdehyde.

TABLE 13 Plasma NO values.

Sample number	Group 1	Group 2	Group 3
1	8.059	12.035	12.389
2	7.469	14.219	15.221
3	9.069	14.099	10.973
4	10.139	10.265	13.097
5	9.169	12.743	14.867
6	9.609	9.912	12.035
7	9.189	10.265	12.389

Abbreviation: NO, nitric oxide.

TABLE 14 Tissue NO values.

Tissue number	Group 1	Group 2	Group 3
1	11.681	24.071	12.389
2	12.389	25.841	11.327
3	15.221	17.345	13.805
4	10.973	20.121	14.513
5	13.097	17.221	15.929
6	14.867	19.469	14.159
7	12.035	18.754	19.469

Abbreviation: NO, nitric oxide.

TABLE 15 Comparison of plasma NO values.

Statistical evaluation of plasma NO values					
Groups	*N*	Average	Standard deviation	Test statistic	Impact
1	7	8.94143	0.917068	$F = 13.438$	0.573
2	7	11.76963	1.762247	$^{*}p = 0.004$ $^{**}p < 0.001$	
3	7	12.78725	1.542325	$^{***}p = 0.369$	

Abbreviation: NO, nitric oxide.

TABLE 16 Comparison of tissue NO values.

Statistical evaluation of tissue NO values					
Groups	*N*	Average	Standard deviation	Test statistic	Impact
1	7	12.89471	1.607450	$F = 16.203$	0.618
2	7	20.12025	3.177043	$^{*}p < 0.001$ $^{**}p = 0.346$	
3	7	14.79663	2.573501	$^{***}p < 0.01$	

Abbreviation: NO, nitric oxide.

($p < 0.005$) was obtained in oxidative stress in tissue samples between the groups.

Paroxanase (PON-1) values measured from plasma and tissue samples are shown in Tables 21 and 22. The means, standard deviations, *p* values, and effect size of PON-1 data of the groups are shown in Tables 23 and 24.

The significant increase in PON-1 activity in the CRV-β-CD group (Table 23) suggests a possible mechanism by which this formulation improves flap survival by enhancing antioxidant defenses.

Plasma values of PON-1, another oxidative stress parameter, are given in Table 23 and tissue values are given in Table 24,

TABLE 17 Plasma SOD values.

Plasma number	Group 1	Group 2	Group 3
1	343.5	370.0	270.4
2	316.3	361.1	305.3
3	322.0	325.3	282.3
4	370.8	300.0	306.8
5	329.0	297.7	352.3
6	290.5	304.2	349.7
7	305.2	319.6	326.8

Abbreviation: SOD, superoxide dismutase.

TABLE 18 Tissue SOD values.

Tissue number	Group 1	Group 2	Group 3
1	471.6	378.9	174.8
2	422.6	403.0	131.3
3	511.7	179.9	184.4
4	527.8	413.2	227.0
5	463.8	158.5	215.8
6	231.2	222.0	159.8
7	475.4	225.9	378.6

Abbreviation: SOD, superoxide dismutase.

TABLE 19 Comparison of plasma SOD values.

Statistical evaluation of plasma SOD value					
Groups	*N*	Average	Standard deviation	Test statistic	Impact
1	7	325.32	26.211	$F = 0.076$ $p = 0.927$	0.008
2	7	326.21	27.241		
3	7	320.7000	35.744		

TABLE 20 Comparison of tissue SOD values.

Istatistical evaluation of tissue SOD value					
Groups	*N*	Average	Standard deviation	Test statistic	Impact
1	7	443.4429	99.570	$F = 10.464$ $p = 0.002$ $^{*}p = 0.008$ $^{**}p = 0.003$ $^{***}p = 0.141$	0.511
2	7	301.0250	114.47979		
3	7	213.1875	75.44335		

Abbreviation: SOD, superoxide dismutase.

and while no statistically significant difference was found between the groups in plasma ($p > 0{,}005$), it was determined that the lowest PON-1 value in tissue samples was in Group 1.

TABLE 21 Plasma PON-1 values.

Plasma number	Group 1	Group 2	Group 3
1	328.5	749.6	710.6
2	318.9	476.5	422.5
3	700.2	613.3	491.5
4	469.8	363.0	450.5
5	448.8	443.2	303.5
6	362.0	358.3	554.9
7	532.3	522.0	401.0

Abbreviation: PON-1, paroxanase.

TABLE 22 Tissue PON-1 values.

Tissue number	Group 1	Group 2	Group 3
1	14.33	14.98	20.45
2	11.44	12.63	30.64
3	14.84	37.20	21.66
4	12.56	17.05	32.22
5	12.38	18.64	29.29
6	18.57	23.10	25.74
7	12.98	21.20	24.70

Abbreviation: PON-1, paroxanase.

TABLE 23 Comparison of plasma PON-1 values.

Statistical evaluation of plasma PON-1 values					
Groups	*N*	Average	Standard deviation	Test statistic	Impact
1	7	451.50	135.05	$F = 0.221$ $p = 0.804$	0.022
2	7	489.70	135.81		
3	7	447.66	144.66		

Abbreviation: PON-1, paroxanase.

TABLE 24 Comparison of tissue PON-1 values.

Statistical evaluation of tissue PON-1 values					
Groups	*N*	Average	Standard deviation	Test statistic	Impact
1	7	13.871	2.376	$F = 8.858$ $p = 0.002$ $^{*}p = 0.133$ $^{**}p = 0.001$ $^{***}p = 0.086$	0.470
2	7	19.677	8.023		
3	7	25.090	7.270		

Abbreviation: PON-1, paroxanase.

2.3.2 | Histopathological examination results

Comparisons of histopathological scoring values of tissue samples between the experimental groups are shown in Figures 9 and 10. When

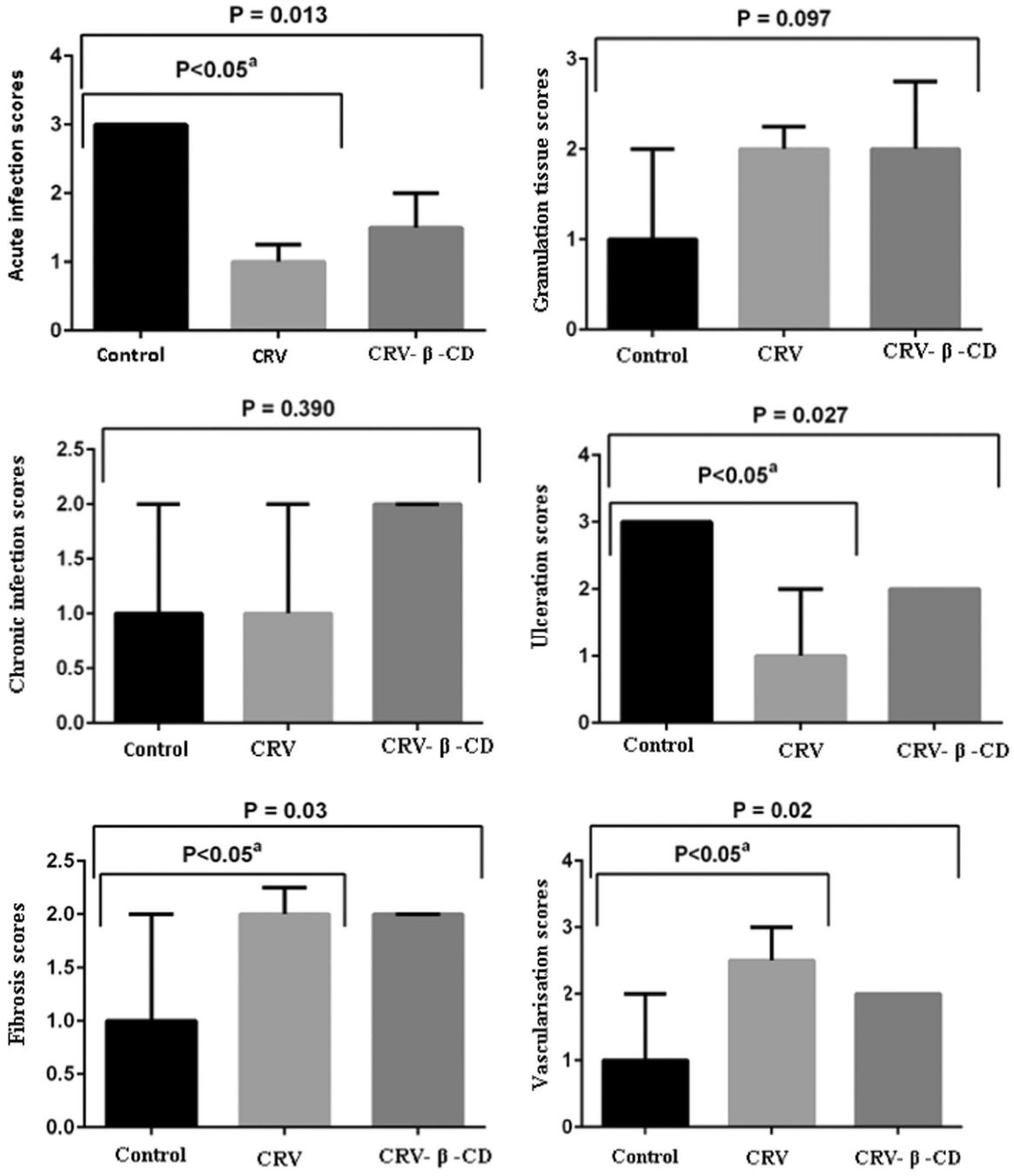

FIGURE 9 Comparison graphs of acute infection, chronic infection, ulceration, granulation, fibrosis, and vascularization values between groups. CRV, carvedilol.

histopathological scoring values were compared between the groups, statistically significant differences were found for acute infection ($p = 0.013$), ulceration ($p = 0.027$), fibrosis ($p = 0.03$), and vascularization ($p = 0.02$) scoring values. There was no statistically significant difference between the groups for chronic infection and granulation scoring values. Our histopathological examination results showed that compared to the control group, CRV treatment significantly decreased acute infection and ulceration ($p < 0.05$) and significantly increased fibrosis and vascularization ($p < 0.05$). When compared with the control group, acute infection, and ulceration were decreased, and fibrosis and vascularization were increased in the CRV-β-CD treated group, but statistical significance was not detected. These results suggest that CRV administration alone was more successful.

3 | DISCUSSION

In the first step of the study, CRV-β-CD inclusion complexes were prepared to increase the bioavailability of CRV by increasing its solubility in water and complex formation was confirmed by FTIR

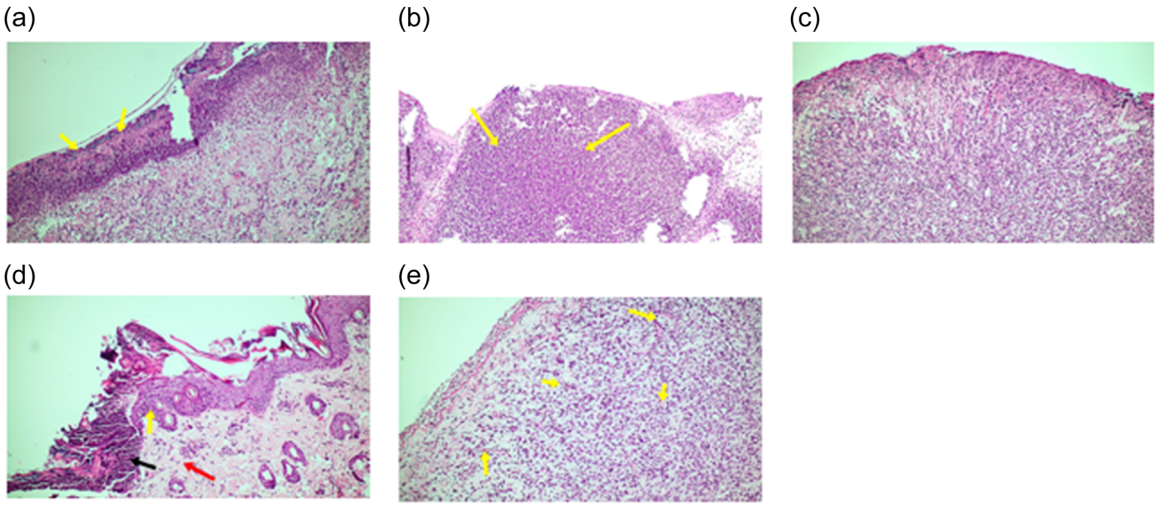

FIGURE 10 Histopathological sections. (a) Dense neutrophil infiltration and ulceration in the tissue sample of the control group. (b) Abscess formation and intense neutrophilic infiltration in the tissue sample of the control group. (c) Intense chronic inflammation and low vascularization in the tissue sample of the control group. (d) Minimal ulceration (black arrow), re-epithelialization (yellow arrow), and chronic inflammation with mild fibrosis (red arrow) in the tissue sample of CRV-treated experimental group. CRV, carvedilol.

analyses. The spectra of the samples taken between the specified wavelengths were different from the free β-CD and CRV. This confirms the formation of the inclusion complex.[14–16] It was determined by solubility study that the solubility of CRV in water increased by 3.14%–5.79% thanks to these complexes. To enhance the solubility of substances in water, inclusion complexes have been prepared, as evidenced by numerous studies.[17–21] This approach has notably increased the solubility of CRV in aqueous solutions. It was determined that the CRV-β-CD complex showing the highest solubility (5.79% increase) was prepared with a molar ratio of 1:3 (CRV:β-CD). CRV ODTs were prepared using the inclusion complexes prepared with this molar ratio and optimized by Box–Behnken experimental design. First order and second order in the formulation design using the Box–Bhenken experimental design, which allows the model coefficients to be estimated effectively, a total of 15 formulations for three factors were tested and economically optimized. When the literature on the subject is examined, it is seen that Box–Behnken experimental design is frequently preferred in many formulation optimizations.[22–24] Because, the Box–Behnken design offers significant advantages in terms of time and cost, particularly in scenarios with many factors, as it requires fewer experiments compared to other experimental designs. Additionally, this design facilitates the creation of second-order models, enabling a deeper understanding of the interactions between factors and the second-order effects of individual factors. Moreover, it reduces the risk of conducting experiments under extreme conditions and enhances practicality by ensuring that all combinations used in the experiments are centered rather than positioned at the corners. According to the ANOVA data of the optimized ODMT formulation, it was determined that only the Parteck ODT® percentage affected the disintegration time of ODTs, while only the magnesium stearate percentage affected the hardness properties of ODTs. It was also determined that the percentage friability values of ODTs were affected by both the Parteck ODT® percentage and the magnesium stearate percentage.

In the second phase of the study, in vivo studies were carried out, considering that CRV formulation with high solubility in flap surgery may reduce oxidative damage. Although planned surgery is performed in flap surgery, there are emergency surgical interventions. These include unexpected situations such as limb amputations, prolonged flap surgery, and vascular insufficiency in the flap. Increasing the solubility and bioavailability with the CD complex may make it possible to intervene more rapidly in I/R injury. For this reason, CRV-β-CD complex was used in our study. In our study, according to the results of drug level analyses, it was shown that the CD complex significantly increased the absorption of CRV. Şentürk et al. investigated the effect of Slimarin on renal ischemia reperfusion injury in their study. In this study, CAT and SOD activities obtained from the homogenate of IRH kidney tissues were found to be higher than the control group, which is not consistent with the existing studies, and they reported that this may be due to the induction of CAT and SOD enzymes during I/R[25,26] evaluated antioxidant markers in muscle, lung, and liver tissues on the seventh day after 4 h of ischemia and 2 h of reperfusion in the experiment in which antioxidant effects of CRV were evaluated on rat hind leg IRH model. In this experiment, CRV pretreatment was given for 10 days and it was observed that it significantly prevented the decrease in tissue SOD and GSH levels caused by I/R.[26] In our study, CRV and CD-linked CRV were started on the same day of surgery and SOD was significantly lower in the CRV-β-CD group compared to the control group and the CRV group. These findings are not consistent with previous studies. In in vitro models, CRV reduced lipid peroxidative damage by scavenging hydroxyl radicals and superoxide anions through the carbazole group.[27] Furthermore, in a study, Christopher et al. showed decreased myeloperoxidase activity, a marker of neutrophil accumulation in splanchnic ischemia and reperfusion-induced

shock and tissue injury.[28] By scavenging oxygen-free radicals, CRV may inhibit the elevation of leukocyte adhesion molecules and thus prevent neutrophil-induced tissue injury. According to our results, CRV group significantly decreased acute infection and ulceration ($p < 0.05$) and significantly increased fibrosis and vascularization ($p < 0.05$). When compared with the control group, acute infection and ulceration decreased, fibrosis and vascularization increased in the CRV-β-CD group, but statistical significance could not be determined. These findings show that CRV application is histologically superior to CRV-CD in tissue healing. Regarding flap viability, it was shown that CRV and CRV-β-CD significantly increased flap viability compared to the control group. Although the flap viability rate of CRV-β-CD was higher than CRV, no significant difference was found between them.

The strength of vasomotility is largely dependent on NO level. NO depletion seen during ischaemiareperfusion process causes vasoconstriction and hypoperfusion.[29] In our study, high NO levels in both the CRV-treated group and the CD-induced CRV group may be related to increased flap survival. Both groups (CRV, CRV-β-CD) significantly increased NO levels in both plasma and tissue compared to the control group.

Another reason for the possible contribution of CRV to flap protection in the I/R model is its selective alpha-1 adrenoreceptor blockade. This effect may lead to direct vasodilatation, resulting in increased blood flow to the ischemic area and thus attenuating ischemic flap injury. PON-1 is a calcium-dependent ester hydrolase with both paraoxonase and arylesterase activity. PON-1 is mainly complex with HDL in human serum and has been shown to protect LDL and HDL from oxidation induced by copper ions or other free radical generators.[30,31] Paraoxonase-1 is an enzyme with three activities, paraoxonase, arylesterase, and diazoxonase, and its activity is inversely correlated with cardiovascular disease (CVD) risk.[32,33] Therefore, PON-1 has been recognized as the key enzyme in HDL responsible for the anti-oxidant effect.[34] The inverse relationship of PON1 with oxidative stress and its ability to protect against oxidation suggest that increasing PON-1 synthesis may be a potential therapeutic target for the treatment of oxidative stress-related diseases, especially CVDs.[35] In our study, PON-1 enzyme activity was measured both in tissue and plasma. Although group 2, in which CRV was used in plasma, increased PON-1 enzyme activity, it was not found significant compared to the control group. However, Group 3, in which CRV-β-CD complex was used, significantly increased PON-1 enzyme activity compared to group 1. The fact that CRV-β-CD increased PON-1 but not CRV may be related to the fact that the treatment started on the same day as ischemia in the experiment. CRV has been shown to increase PON-1 level in other studies.[36] This suggests that the CD complex does its job and increases bioavailability, and that this complex given on the same day in flap surgery may reduce oxidative damage and increase flap viability. As a result, the study's results align with previous research showing the benefits of CRV in reducing I/R injury and further highlight the enhanced efficacy of its ODT formulation in promoting flap viability. Furthermore, these findings suggest that carvedilol ODTs may be a viable option to improve outcomes in flap surgeries, particularly in cases where rapid onset of action is important. Future clinical studies may confirm these findings in human subjects.

4 | CONCLUSİON

In this study, we investigated the effects of CRV ODTs on I/R injury and flap viability in a rat model. The study aimed to enhance the pharmacological efficacy of CRV by formulating it into ODTs, which offer rapid disintegration and improved bioavailability. The study consisted of both in vitro and in vivo evaluations to understand the vasodilatory and antioxidant properties of CRV in mitigating I/R injury. The in vitro studies demonstrated that the CRV-β-CD inclusion complex significantly increased the solubility of CRV, facilitating its formulation into ODTs. The optimization of ODT formulations using the Box–Behnken experimental design provided tablets with favorable disintegration time, hardness, and friability, which are critical parameters for effective drug delivery. In the in vivo experiments, rats were subjected to I/R injury, and the effects of CRV and CRV ODT were compared to a control group. The results indicated that both CRV and its ODT formulation significantly improved flap viability compared to the control group. Biochemical analysis revealed that the CRV-β-CD complex notably increased the levels of NO and PON-1, which are associated with improved vascular function and antioxidant defense. Histopathological examination showed that CRV treatment reduced acute infection and ulceration while enhancing fibrosis and vascularization. The CRV-β-CD complex, while effective, did not achieve the same level of histological improvement as CRV alone. These findings suggest that CRV, particularly in its ODT form, can offer substantial protective effects against I/R injury, improving flap survival and tissue healing.

CRV ODTs offer a promising strategy for enhancing flap viability in plastic surgery.

The successful formulation of CRV into ODTs represents a significant advancement in the management of I/R injury. This approach may be particularly beneficial in clinical scenarios that require fast-acting treatments to enhance flap viability. Further clinical studies are warranted to confirm these findings and explore the potential of CRV ODTs in plastic and reconstructive surgery.

5 | EXPERIMENTAL

CRV was gifted by Santa Farma (Türkiye) pharmaceutical company, β-CD (Sigma-Aldrich), hydrochloric acid (Sigma-Aldrich), mannitol (Merck), Parteck ODT® (Merck), Avicel PH 101® (Sigma-Aldrich), magnesium stearate (Sigma-Aldrich), Phosphate buffer solutions (Sigma-Aldrich), Sprague–Dawley Female Rats (Saki Yenilli Experimental Animals Production and Application Laboratory Tic. Ltd.), UV/VIS spectrophotometer (Shimadzu UV-1800), and talc (Sigma-Aldrich). All solvents were supplied analytical grade by Sigma-Aldrich.

5.1 | Methods

5.1.1 | Determination of the calibration equation for CRV using UV spectrophotometric method

A stock solution of CRV was prepared in methanol:0.1 N HCl (10:90) at a concentration of 10 mg/100 mL. Subsequently, solutions were prepared at concentrations of 5, 10, 15, 20, 25, 30, and 35 µg/mL based on this stock solution. Upon obtaining the spectrum from the solution with a concentration of 15 µg/mL, it was determined that the wavelength at which maximum absorbance occurred was 240 nm. The absorbance values obtained from the solutions, the calibration curve, and the corresponding equation are presented.

5.1.2 | Preparation and characterization studies of CRV-β-CD inclusion complexes

Preparation of CRV-β-CD inclusion complexes

To enhance the solubility of CRV, classified under BCS Class II, inclusion complexes with β-CD were prepared using the kneading method, employing an ethanol:water (2:1) solvent system. CRV and β-CD were mixed in 1:1, 1:2, and 1:3 molar ratios (CRV:β-CD). The combined mixture was kneaded in a mortar with the assistance of the solvent until a dough-like consistency was achieved. The resulting mass was passed through a No. 2 sieve and dried at 50°C. The dried mass was then further homogenized by passing it through a No. 1 sieve to ensure uniform particle size.[37–39]

Characterization of CRV-β-CD inclusion complexes

Determination of FTIR spectra. The FTIR spectra of the prepared complexes were obtained using a Perkin Elmer (USA) instrument.

Determination of the solubilities of the inclusion complex in aqueous medium. CRV-β-CD inclusion complexes at ratios of 1:1, 1:2, and 1:3 were obtained in excess and placed in 10 mL of a 0.1 N HCl solution. The mixture was then shaken at 100 rpm in a water bath at 25°C for 48 h. After this period, each sample was centrifuged at 4000 rpm for 5 min, and the absorbance values at 240 nm of the supernatant samples were determined triplicately using a spectrophotometer. The obtained absorbance values were substituted into the correct equation to calculate the amount of dissolved CRV.[40,41]

Preparation and optimization of carvedilol-β-CD ODT formulations according to Box–Behnken experimental design. ODTs were prepared in two replicates, containing Ac-Di-Sol®, mannitol, Avicel PH 101®, talc, and magnesium stearate, as well as CRV-β-CD (CRV-β-CD) inclusion complex and were optimized with the experimental design. ADT formulations have been shown in Table 25.

TABLE 25 ODT formulations.

	%					
	CRV-β-CD inclusion complex (1:3) (amount of complex equivalent to 5 mg CRV)	Mannitol	Parteck ODT®	Avicel® PH 101	Talc	Magnesium stearate
F1	35.38	30	15	8.12	10	1.5
F2	35.38	25	5	23.62	10	1
F3	35.38	30	5	18.12	10	1.5
F4	35.38	25	10	18.12	10	1.5
F5	35.38	35	10	8.12	10	1.5
F6	35.38	30	10	13.62	10	1
F7	35.38	35	15	3.62	10	1
F8	35.38	35	5	13.62	10	1
F9	35.38	30	5	19.12	10	0.5
F10	35.38	25	10	19.12	10	0.5
F11	35.38	35	10	9.12	10	0.5
F12	35.38	30	10	13.62	10	1
F13	35.38	25	15	13.62	10	1
F14	35.38	30	15	9.12	10	0.5
F15	35.38	30	10	13.62	10	1

Physicochemical properties of CRV ODTs

In the study, the three most important physicochemical properties of ODT formulations, disintegration time, hardness, and friability values, were taken into consideration, and these three parameters were accepted as dependent variables.[42–44] Since the optimization of ODTs will be done with the Box–Behnken experimental design, the percentage mannitol, superdisintegrant (Parteck ODT®), and lubricant (magnesium stearate) values used were determined as independent variables.[22,45] The effect of independent variables on dependent variables was evaluated statistically.

Analytical method development and validation for CRV analysis from biological material

Analytical conditions and stock solutions. The AdSDPV was developed using an AUTOLAB/PGSTAT-30 electrochemical analysis system and GPES 4.9 software package (Eco Chemie) for the quantification of CRV. A platinum wire counter electrode, an Ag/AgCl reference electrode, and a glassy carbon (GC) working electrode (3 mm diameter) were used in three-electrode voltammetric cells. Phosphate buffer solutions with different pH values (pH 2.0–4.0 and pH 6.0–8.0) were freshly prepared and stored in the refrigerator. The stock solution of CRV was prepared in methanol at concentration of 70.85 µg/mL. The working solutions were obtained by diluting the stock solutions with pH 8.02 phosphate buffer solution.[46,47] The optimum conditions were examined for AdSDPV: step potential, 0.01 V, modulation amplitude, 0.05 V, modulation time, 0.05 s, interval time, 0.5 s, deposition potentials, 0.2 V and 0.6 V, and deposition time, 2400 s.

Calibration standards and bioanalytical method validation. The rat serum samples ($n = 21$), obtained from Sprague–Dawley female rats (Groups I–III), were stored at −80°C until electroanalysis. The blank rat serum (Group I) was employed for the development of the voltammetric method. The calibration solutions were prepared by diluting the 70.85 µg/mL CRV stock solutions with blank rat serum (Group I) in serum:methanol ratio of 1/5 (v/v). The prepared solutions were mixed in an ultrasonic bath for 5 min and centrifuged at 9000 rpm for 30 min at 4°C. The clear supernatant of the serum samples were diluted with pH 8.02 phosphate buffer solution in serum/buffer ratio of 55/45 (v/v) to obtain the calibration concentration range from 0.17 to 0.34 µg/mL. These calibration solutions were directly measured by AdSDPV without any time-consuming sample preparation step, and the calibration curve was given with correlation coefficient (r).[48]

The recovery studies were realized to estimate the accuracy by addition of pure CRV into the rat serum matrix. Percentage of recovery was calculated by using the calibration regression data. The precision of the method was analyzed within 1 day for assessing intra-day, and 5 days for assessing inter-day variability ($n = 3$). The relative standard deviations (RSDs) were calculated for intra-day and inter-day precision. LOD and LOQ are determined according to ICH guidelines (LOD = 3 s/m; LOQ = 10 s/m where "s" is the standard deviation of the lowest concentration response and m is the slope of the calibration line.).[49]

Analysis of serum samples. The developed AdSDPV method was applied to Groups II and III rat serums for the quantification of CRV. Group II (only applied CRV) and Group III (applied CRV-β-CD Inclusion Complexes) rat serum samples were diluted with methanol in serum:methanol ratio of 1:5 (v:v). The prepared solutions were mixed in an ultrasonic bath and centrifuged as previous conditions. The clear supernatant of the serum samples was diluted with phosphate buffer solution as previous ratio. The content of CRV for Groups II and III rat serums were calculated by using the calibration curve. One-way analysis of variance (ANOVA) and post hoc (Tukey test) were performed. The significance was determined at $p < 0.05$ and $p < 0.01$.[50]

In vivo experiments using Sprague–Dawley female rats (n = 21)

Our study was designed as a prospective randomized controlled in vivo animal experiment. A total of 24 Sprague–Dawley rats were used in the experiment. In this study, 24 male Sprague–Dawley rats weighing 400–500 g, 20 weeks old, were kept individually in a standard cage specially designed for rats for 7 days at a temperature of 21–24°C and an air humidity of 50%. Rats had ad libitum access to food and water throughout the study, while light and dark cycles were automatically regulated in 12-h periods. In the study, the experimental animals were divided into groups as Group 1 (control group), Group 2 (Group A), and Group 3 (Group B).[12,51] A total of 24 Sprague–Dawley rats were divided into three groups of eight, with each group receiving different treatments as described below.

First group. It was considered as the control group. The rats were given 10 cc saline 2 h before the experiment. A 6 × 3 cm^2 inferior epigastric artery flap was planned from the left inguinal region. In accordance with this plan, the circulation of the inferior epigastric artery was stopped with a microclamp for 8 h after the flap was eluted. At the eighth hour, the microclamp was opened and the flap was adapted with 3/0 silk suture. The rats were fed ad libitum with food and water for 7 days after the operation and sacrificed on the seventh day of the operation and tissue samples were taken.

Second group. CRV (2 mg/kg) was administered by oral gavage 2 h before the start of the experiment to this group of rats designated as Group A. A 6 × 3 cm^2 inferior epigastric artery flap was planned from the left inguinal region. In accordance with this plan, the circulation of the inferior epigastric artery was stopped with a microclamp for 8 h after the flap was eluted. At the eighth hour, the microclamp was opened and the flap was adapted with 3/0 silk suture. The rats were fed ad libitum with food and water for 7 days after the operation. On the seventh day of the operation, CRV (2 mg/kg) was given to the rats by oral gavage 1 h before tissue samples were taken and then sacrificed and tissue samples were taken.

Third group. This group of rats, designated as group B, was administered 2 mg/kg CD-linked CRV by oral gavage 2 h before the

experiment. A $6 \times 3\ cm^2$ inferior epigastric artery flap was planned from the left inguinal region. In accordance with this plan, the circulation of the inferior epigastric artery was stopped with a microclamp for 8 h after the flap was eluted. At the eighth hour, the microclamp was opened and the flap was adapted with 3/0 silk suture. The rats were fed ad libitum with food and water for 7 days after the operation. On the seventh day of the operation, ODTs containing CRV-CD inclusion complex (2 mg/kg) were administered by oral gavage 1 h before tissue samples were taken, then the rats were sacrificed and tissue samples were taken.

Rat inferior epigastric artery skin flap model. A rat inferior epigastric artery skin flap model, measuring $3 \times 6\ cm^2$, will be employed to simulate the surgical context. This model will serve as the platform for assessing the impact of CRV and its ODT form on flap viability during I/R challenges. The analytical methods validated for in vitro characterization will be applied to analyze samples collected from the rat flap model, ensuring the accuracy and reliability of the obtained results.

Taking tissues and blood for biochemical and histopathological examination. On the seventh postoperative day, approximately $1 \times 1\ cm^2$ of tissue (at least 0.1 g) was excised from the inferior epigastric artery skin island flap for biochemical evaluation of the tissue after sacrification. These tissues were homogenized and MDA, NO, SOD, and PON-1 were analyzed. The remaining tissue was preserved in formaldehyde solution for histopathological examination.

In the study, MDA was measured by reaction with thiobarbituric acid (TBA) in the temperature range of 90–100°C. With maximum absorption at 532 nm, a pink pigment formation is observed between MDA or MDA-like substances and TBA in the TBA test reaction. For 15 min, the reaction was carried out in the pH 2–3 range and at 90°C. The sample was mixed with cold 10% (w/v) trichloroacetic acid to precipitate the protein. The pelleted precipitate was separated by centrifugation and a sample of the supernatant was reacted in an equal volume of boiling water bath containing 0.67% (w/v) TBA. After cooling, the absorbance was measured at a wavelength of 532 nm.[52,53]

NO can easily be oxidized to NO_2 (nitrogen dioxide) in living organisms or in aqueous solution, forming a red azo compound with a color-developing agent. The concentration of this nitrogen compound is linearly related to the NO concentration. In the study, the NO concentration was calculated indirectly by measuring the optical density (OD) at 550 nm.[54,55]

SOD contributes to the protection of cells and tissues by rapidly decomposing hydrogen peroxide and molecular oxygen, which are harmful molecules formed during oxidative energy production. In the approach used, xanthine and xanthine oxidase are used to generate superoxide radicals, which then interact with 2-(4-iodophenyl)-3-(4-nitrophenol)-5-phenyltetrazolium chloride to form a red formazan dye. The level of inhibition of this reaction was used to measure superoxide dismutase activity.[56]

PON-1 enzyme activity was measured using commercially available kits (Relassay). The rate of paraoxon hydrolysis (diethyl pnitrophenyl phosphate) was measured by monitoring the increase in absorption at 412 nm at 37°C.[57,58]

Histopathological examination. Tissue samples were fixed in 10% formaldehyde solution, embedded in paraffin, and 4-µm-thick sections were prepared. After deparaffinisation and gradual hydration, the sections were stained with haematoxylin-eosin (H&E) and examined under a light microscope (Olympus BX41) by a pathologist who was not familiar with the study groups.[59,60]

Statistical analysis

The SPSS program (IBM Corp., 2015 release. IBM SPSS for Mac OS, v23.0) was used for statistical analysis. For continuous data, the mean ± standard deviation was calculated as descriptive statistics. For comparative analysis, Student's *t* test or one-way ANOVA was applied to parametric data sets, while the Mann–Whitney *U* test and Kruskal–Wallis test were used for nonparametric data sets. In post hoc comparisons, Tukey's test was employed for ANOVA results, and Bonferroni correction along with Dunn's post hoc test was applied for Kruskal–Wallis results. The Shapiro–Wilk test, histograms, kurtosis/skewness measurements, and adjusted *Q*–*Q* plots were used to assess the normality of the data. Homogeneity of variances was evaluated using Levene's test. Statistical significance was set at $p = 0.05$, and appropriate revisions were made in comparisons using Bonferroni correction.[60]

ACKNOWLEDGMENTS

This research did not receive any specific grant from funding agencies in the public, commercial, or not-for-profit sectors.

DATA AVAILABILITY STATEMENT

The data that supports the findings of this study are available in the Supporting Information of this article.

ORCID

Serkan Tokgonul http://orcid.org/0009-0005-6221-7584
Emine Dilek Ozyilmaz http://orcid.org/0000-0002-1791-3055
Tansel Comoglu http://orcid.org/0000-0002-4221-5814
Manolya Müjgan Gürbüz http://orcid.org/0009-0005-9170-5536
Burcu Doğan Topal http://orcid.org/0000-0002-6455-4577
Fatma Emel Kocak http://orcid.org/0000-0001-5549-3883
Hülda Rıfat Ozakpinar http://orcid.org/0000-0001-7071-367X

REFERENCES

[1] J. R. Sanger, *Plast. Reconstr. Surg.* **2018**, *141*(1), 245.
[2] E. Martinez-Hernandez, G. Kanaporis, L. A. Blatter, *Channels* **2022**, *16*(1), 97.
[3] T. Benkel, M. Zimmermann, J. Zeiner, S. Bravo, N. Merten, V. J. Y. Lim, E. S. F. Matthees, J. Drube, E. Miess-Tanneberg, D. Malan, M. Szpakowska, S. Monteleone, J. Grimes, Z. Koszegi, Y. Lanoiselée, S. O'Brien, N. Pavlaki, N. Dobberstein, A. Inoue, V. Nikolaev, D. Calebiro, A. Chevigné, P. Sasse, S. Schulz, C. Hoffmann, P. Kolb, M. Waldhoer, K. Simon, J. Gomeza, E. Kostenis, *Nat. Commun.* **2022**, *13*(1), 7109.

[4] M. I. Ragone, M. Bayley, G. A. Colareda, P. Bonazzola, A. E. Consolini, *J. Cardiovasc. Pharmacol. Ther*. **2020**, *25*(1), 72.
[5] J. I. Park, M. S. Jung, H. Lee, H. Kim, J. Oh, *Braz. J. Anesthesiol*. **2022**, *72*, 152.
[6] J. P. Rubin, P. C. Neligan, *Plastic Surgery: Volume 2: Aesthetic Surgery*, Elsevier Health Sciences, Amsterdam **2017**.
[7] W. G. S. Bonservizi, M. K. Koike, R. Saurim, G. A. A. Felix, S. M. da Silva, E. F. S. Montero, M. O. Taha, *Transplant. Proc*. **2014**, *46*(6), 1862.
[8] M. Ovize, H. Thibault, K. Przyklenk, *Circ. Res*. **2013**, *113*(4), 439.
[9] T. Comoglu, E. Dilek Ozyilmaz, *Pharm. Dev. Technol*. **2019**, *24*(7), 902.
[10] M. P. Ghourichay, S. H. Kiaie, A. Nokhodchi, Y. Javadzadeh, *BioMed Res. Int*. **2021**, *2021*, 1.
[11] T. Comoglu, F. Bahadori. 18 Granulation and Production Approaches of Orally Disintegrating Tablets, **2021**.
[12] S. H. Min, S. H. Choe, W. S. Kim, S. H. Ahn, Y. J. Cho, *Sci. Rep*. **2022**, *12*(1), 8130.
[13] R. Khalaf, D. Duarte Bateman, J. Reyes, D. Najafali, A. Rampazzo, B. Bassiri Gharb, *Microsurgery* **2024**, *44*(2), e31141.
[14] G. Paladini, F. Caridi, V. Crupi, F. De Gaetano, D. Majolino, S. Tommasini, C. A. Ventura, V. Venuti, R. Stancanelli, *Molecules* **2021**, *26*(12), 3749.
[15] X. Han, Z. Zhang, H. Shen, J. Zheng, G. Zhang, *Food Res. Int*. **2019**, *125*, 108619.
[16] S. Alshehri, S. S. Imam, A. Hussain, M. A. Altamimi, *Processes* **2020**, *8*(11), 1450.
[17] D. Sid, M. Baitiche, Z. Elbahri, F. Djerboua, M. Boutahala, Z. Bouaziz, M. Le Borgne, *J. Enzyme Inhib. Med. Chem*. **2021**, *36*(1), 605.
[18] P. Mahalapbutr, P. Wonganan, T. Charoenwongpaiboon, M. Prousoontorn, W. Chavasiri, T. Rungrotmongkol, *Biomolecules* **2019**, *9*(10), 545.
[19] S. Gao, J. Y. Jiang, Y. Y. Liu, Y. Fu, L. X. Zhao, C. Y. Li, F. Ye, *Polymers* **2019**, *11*(9), 1396.
[20] B. R. Giri, J. Lee, D. Y. Lim, D. W. Kim, *Drug Dev. Ind. Pharm*. **2021**, *47*(2), 319.
[21] G. M. Tawfik, K. A. S. Dila, M. Y. F. Mohamed, D. N. H. Tam, N. D. Kien, A. M. Ahmed, *Trop. Med. Health* **2019**, *47*, 1.
[22] A. K. Chettupalli, P. A. Rao, M. Kuchukuntla, V. Bakshi, *Res. J. Pharm. Technol*. **2020**, *13*(12), 6195.
[23] A. Kundawala, P. Patel, K. Chauhan, A. Desai, D. Kapadia, *J. Drug Delivery Ther*. **2019**, *9*(4–A), 86.
[24] P. K. Kumari, K. Srilekhya, M. S. S. Vastav, **2022**.
[25] C. E. Berry, T. Le, N. An, M. Griffin, M. Januszyk, C. B. Kendig, A. Z. Fazilat, A. A. Churukian, P. M. Pan, D. C. Wan, *J. Transl. Med*. **2024**, *22*(1), 68.
[26] H. Chen, T. Zhang, S. Yan, S. Zhang, Q. Fu, C. Xiong, L. Zhou, X. Ma, R. Wang, G. Chen, *Heliyon* **2024**, *10*(9), e29874.
[27] A. Cargnoni, C. Ceconi, P. Bernocchi, A. Boraso, S. Curello, R. Ferrari, *Eur. J. Heart Fail*. **2000**, *2*, 6.
[28] T. A. Christopher, B. L. Lopez, X. L. Ma, G. Z. Feuerstein, R. R. Ruffolo, Jr., T. L. Yue, *Br. J. Pharmacol*. **1998**, *123*(2), 292.
[29] R. Mittermayr, D. Valentini, F. Fitzal, S. Hallström, H. Gasser, H. Redl, *Wound Repair Regen*. **2003**, *11*(1), 3.
[30] A. D. Watson, J. A. Berliner, S. Y. Hama, B. N. La Du, K. F. Faull, A. M. Fogelman, M. Navab, *J. Clin. Invest*. **1995**, *96*(6), 2882.
[31] M. Aviram, M. Rosenblat, C. L. Bisgaier, R. S. Newton, S. L. Primo-Parmo, B. N. La Du, *J. Clin. Invest*. **1998**, *101*(8), 1581.
[32] A. Canales, F. J. Sánchez-Muniz, *Med. Clín*. **2003**, *121*(14), 537.
[33] G. S. Getz, C. A. Reardon, *Curr. Opin. Lipidol*. **2004**, *15*(3), 261.
[34] M. C. Blatter, R. W. James, S. Messmer, F. Barja, D. Pometta, *Eur. J. Biochem*. **1993**, *211*(3), 871.
[35] M. Gur, M. Aslan, A. Yildiz, R. Demirbag, R. Yilmaz, S. Selek, O. Erel, I. Ozdogru, *Eur. J. Clin. Invest*. **2006**, *36*(11), 779.
[36] S. Ayashi, A. Assareh, M. Jalali, S. Olapour, H. Yaghooti, *Indian J. Pharmacol*. **2016**, *48*(4), 372.
[37] S. Rigaud, D. Mathiron, T. Moufawad, D. Landy, F. Djedaini-Pilard, F. Marçon, *Pharmaceutics* **2021**, *13*(11), 1746.
[38] S. Chandra, S. Sangeetha, S. Kavibharathi, B. Nandhini, R. Suresh, C. Sanjeevkumar, **2020**.
[39] A. G. Bakr, E. H. M. Hassanein, F. E. M. Ali, E. A. M. El-Shoura, *Life. Sci*. **2022**, *311*, 121152.
[40] D. Csicsák, E. Borbás, S. Kádár, P. Tőzsér, P. Bagi, H. Pataki, B. Sinkó, K. Takács-Novák, G. Völgyi, *New J. Chem*. **2021**, *45*(26), 11618.
[41] B. J. Boyd, C. A. S. Bergström, Z. Vinarov, M. Kuentz, J. Brouwers, P. Augustijns, M. Brandl, A. Bernkop-Schnürch, N. Shrestha, V. Préat, A. Müllertz, A. Bauer-Brandl, V. Jannin, *Eur. J. Pharm. Sci*. **2019**, *137*, 104967.
[42] J. Szlęk, M. H. Khalid, A. Pacławski, N. Czub, A. Mendyk, *Pharmaceutics* **2022**, *14*(4), 859.
[43] E. Tashan, A. Karakucuk, N. Celebi, *AAPS PharmSciTech* **2020**, *21*, 1.
[44] E. D. Özyılmaz, T. Comoglu, *Drug Dev. Ind. Pharm*. **2022**, *48*(11), 667.
[45] M. M. A. Elsayed, M. O. Aboelez, B. E. M. Elsadek, H. A. Sarhan, K. A. Khaled, A. Belal, A. Khames, Y. A. Hassan, A. A. Abdel-Rheem, E. B. Elkaeed, M. Raafat, M. Elsadek, *Pharmaceutics* **2022**, *14*(4), 880.
[46] M. F. de Carvalho, L. F. Garcia, I. Y. L. de Macedo, R. N. Marreto, M. T. de Oliveira, R. O. do Couto, C. E. P. da Cunha, K. C. de Siqueira Leite, K. R. Rezende, F. B. Machado, V. Somerset, E. Gil, *Pharmaceuticals* **2020**, *13*(4), 70.
[47] A. K. Ateş, E. Er, H. Çelikkan, N. Erk, *Microchem. J*. **2019**, *148*, 306.
[48] E. Güven, F. Öztürk, *Hittite J. Sci. Eng*. **2023**, *10*(1), 43.
[49] European Medicines Agency, 2006.
[50] M. R. J. Sarvestani, T. Madrakian, A. Afkhami, *J. Electroanal. Chem*. **2021**, *899*, 115666.
[51] M. Iwaki, T. Niwa, H. Tanaka, A. Kawase, H. Komura, *J. Pharm. Pharm. Sci*. **2019**, *22*, 72.
[52] D. A.Cherian, T. Peter, A. Narayanan, S. S. Madhavan, S. Achammada, G. P. Vynat, *J. Pharm. BioAllied Sci*. **2019**, *11*, S297.
[53] C. Mas-Bargues, C. Escrivá, M. Dromant, C. Borrás, J. Viña, *Arch. Biochem. Biophys*. **2021**, *709*, 108941.
[54] J. Yu, M. Li, D. Zhan, C. Shi, L. Fang, C. Ban, X. Tang, *Pharmacogn. Mag*. **2020**, *16*(72), 836–842.
[55] F. Leo, T. Suvorava, S. K. Heuser, J. Li, A. LoBue, F. Barbarino, E. Piragine, R. Schneckmann, B. Hutzler, M. E. Good, B. O. Fernandez, L. Vornholz, S. Rogers, A. Doctor, M. Grandoch, J. Stegbauer, E. Weitzberg, M. Feelisch, J. O. Lundberg, B. E. Isakson, M. Kelm, M. M. Cortese-Krott, *Circulation* **2021**, *144*(11), 870.
[56] R. Zameer, K. Fatima, F. Azeem, H. I. M. ALgwaiz, M. Sadaqat, A. Rasheed, R. Batool, A. N. Shah, M. Zaynab, A. A. Shah, K. A. Attia, M. AlKahtani, S. Fiaz, *Front. Plant Sci*. **2022**, *13*, 870241.
[57] R. Campagna, V. Pozzi, S. Giorgini, D. Morichetti, G. Goteri, D. Sartini, E. N. Serritelli, M. Emanuelli, *Hum. Cell* **2023**, *36*(3), 1108.
[58] S. Fumarola, M. Cecati, D. Sartini, G. Ferretti, G. Milanese, A. B. Galosi, V. Pozzi, R. Campagna, C. Morresi, M. Emanuelli, T. Bacchetti, *Antioxidants* **2020**, *9*(2), 175.
[59] C. Ceccopieri, J. Skonieczna, J. P. Madej, *J. Vet. Res*. **2021**, *65*(1), 125.
[60] S. El Zein, O. Boccara, V. Soupre, A. F. Vieira, C. Bodemer, A. Coulomb, M. Wassef, S. Fraitag, *Histopathology* **2020**, *77*(2), 275.

How to cite this article: S. Tokgonul, E. D. Ozyilmaz, T. Comoglu, M. M. Gürbüz, B. Doğan Topal, F. E. Kocak, H. R. Ozakpinar, *Arch. Pharm*. **2024**;*357*:e2400618. https://doi.org/10.1002/ardp.202400618